

2005

# Long distance effects and strangeness in the nucleon

John Donoghue

*University of Massachusetts - Amherst*, donoghue@physics.umass.edu

Barry Holstein

holstein@physics.umass.edu

Tobias Huber

Andreas Ross

Follow this and additional works at: [http://scholarworks.umass.edu/physics\\_faculty\\_pubs](http://scholarworks.umass.edu/physics_faculty_pubs)



Part of the [Physics Commons](#)

---

## Recommended Citation

Donoghue, John; Holstein, Barry; Huber, Tobias; and Ross, Andreas, "Long distance effects and strangeness in the nucleon" (2005). *Fizika B*. 256.

[http://scholarworks.umass.edu/physics\\_faculty\\_pubs/256](http://scholarworks.umass.edu/physics_faculty_pubs/256)

This Article is brought to you for free and open access by the Physics at ScholarWorks@UMass Amherst. It has been accepted for inclusion in Physics Department Faculty Publication Series by an authorized administrator of ScholarWorks@UMass Amherst. For more information, please contact [scholarworks@library.umass.edu](mailto:scholarworks@library.umass.edu).

# Long distance effects and strangeness in the nucleon

John F. Donoghue<sup>a</sup>, Barry R. Holstein<sup>a</sup>,  
Tobias Huber<sup>a,b,c</sup> and Andreas Ross<sup>a,b</sup>

<sup>a</sup> Department of Physics-LGRT  
University of Massachusetts  
Amherst, MA 01003

<sup>b</sup> Institut für Theoretische Teilchenphysik  
Universität Karlsruhe  
Karlsruhe, Germany

<sup>c</sup> Institut für Theoretische Physik  
Universität Zürich  
Zürich, Switzerland

February 2, 2008

## Abstract

We discuss the calculation of the strange magnetic radius of the proton in chiral perturbation theory. In particular we investigate the low energy component of the loop integrals involving kaons. We separate the chiral calculation into a low energy part and a high energy component through use of a momentum space separation scale. This separation shows that most of the chiral calculation comes from high energies where the effective field theory treatment is not valid. The resulting low energy prediction is in better agreement with dispersive treatments. Finally, we briefly discuss magnetic moments and show how our techniques can help resolve an old puzzle in understanding the magnetic moments of the proton and  $\Sigma^+$ .

# 1 Introduction

In this paper, we re-examine the issue of strangeness components in the nucleon wavefunction. Although the valence quarks in the neutron and proton are non-strange, the nucleons can acquire matrix elements of strange currents through virtual effects. One traditional way to estimate such effects is through kaon loops in the framework of chiral perturbation theory. At first sight this seems quite appealing as chiral perturbation theory provides a rigorous treatment of the Goldstone bosons as an expansion in the energy and the masses of the quarks. However, it is becoming clearer that the strange quark mass (and hence the kaon mass) is too large for a reliable effective field theory treatment in the baryon sector. In this paper we address one of the cleanest measures of strangeness—the strange magnetic radius—as well as some related quantities, and we discuss the reliability of the effective field theory treatment.

The strange magnetic radius is one of those special quantities in chiral perturbation theory that is finite at one loop without requiring any contributions from low energy constants in the chiral Lagrangian. The one loop result then represents a unique parameter-free contribution[1]. However, the chiral prediction is in strong contradiction with the corresponding dispersive calculation, which finds a much smaller answer[2]. Part of the motivation for the present work is to attempt to elucidate this discrepancy. On the experimental side the only experiment which focuses on the strange magnetic form factor is SAMPLE, which was performed at MIT-Bates at a momentum transfer  $q^2 = -0.1 \text{ GeV}^2$  [3]. There exist also forward experiments—HAPPEX [4] and G0 [5] at JLab and PVA4 at Mainz [6]—which measure a linear combination of strange magnetic and charge radius effects, but the statistical precision is not yet sufficient to produce a meaningful experimental value for the slope of strange magnetism, so our conclusions will be based only on theoretical calculation.

An effective field theory is a technique for exploring the long-distance/low-energy predictions of a more complete full theory. For mesonic chiral perturbation theory, the separation between low-energy and high-energy often occurs around 700 MeV, when the rho meson becomes important. In the dispersive approach, the  $K\bar{K}$  cut in the t-channel starts at an energy  $s = 4m_K^2 \sim 1 \text{ GeV}^2$ . For scales below this separation energy the effective field theory description can be taken as reliable, while above this value new degrees of freedom come into play and the effective treatment can no longer be trusted. This leads us to question how much of the chiral kaon loop actually comes from the long distance regime and is therefore reliably

predicted. We will address this issue specifically below and show that almost all of the chiral prediction for the strange magnetic radius comes from short distances, where the effective field theory is no longer believable.

## 2 Notation

The calculation of baryon magnetic moments and the strange magnetic radius requires the chiral Lagrangians given below, where we follow closely [1].

$$\mathcal{L}_{MM} = \frac{F_\phi^2}{4} \text{Tr} \left( D_\mu U (D^\mu U)^\dagger \right) + \frac{F_\phi^2}{4} \text{Tr} \left( \chi U^\dagger + U \chi^\dagger \right) \quad (1)$$

$$\mathcal{L}_{MB} = \text{Tr}(\bar{B} i v \cdot DB) + D \text{Tr}(\bar{B} S^\mu \{u_\mu, B\}) + F \text{Tr}(\bar{B} S^\mu [u_\mu, B]) \quad (2)$$

with

$$D_\mu U = \partial_\mu U - i \left[ v_\mu^{(i)}, U \right] + \dots \quad (3)$$

$$U = u^2 = \exp \left( i \sqrt{2} \Phi / F_\phi \right) \quad (4)$$

$$D_\mu B = \partial_\mu B + [\Gamma_\mu, B] - i B \text{Tr} \left( v_\mu^{(0)} \right) \quad (5)$$

$$\Gamma_\mu = \frac{1}{2} [u^\dagger, \partial_\mu u] - \frac{i}{2} u^\dagger v_\mu^{(i)} u - \frac{i}{2} u v_\mu^{(i)} u^\dagger + \dots \quad (6)$$

$$u_\mu = i u^\dagger (D_\mu U) u^\dagger \quad (7)$$

Furthermore, we use  $D = 3/4$  and  $F = 1/2$  for the meson-baryon couplings and  $F_\phi = (F_\pi + F_K)/2 \simeq 102$  MeV for the average pseudoscalar decay constant.  $\text{Tr}$  denotes the trace in flavor space and  $S_\mu = \frac{i}{2} \gamma_5 \sigma_{\mu\nu} v^\nu$  is the Pauli-Lubanski spin vector [16].  $v_\mu^{(0)}$  stands for the singlet current whereas  $v_\mu^{(i)}$ ,  $i = 1 \dots 8$ , stands for the  $i$ -th component of the octet current. The meson and baryon fields are contained in the two matrices

$$\Phi = \begin{pmatrix} \frac{\eta}{\sqrt{6}} + \frac{\pi^0}{\sqrt{2}} & \pi^+ & K^+ \\ \pi^- & \frac{\eta}{\sqrt{6}} - \frac{\pi^0}{\sqrt{2}} & K^0 \\ K^- & \bar{K}^0 & -\frac{2\eta}{\sqrt{6}} \end{pmatrix} \quad B = \begin{pmatrix} \frac{\Lambda}{\sqrt{6}} + \frac{\Sigma^0}{\sqrt{2}} & \Sigma^+ & p \\ \Sigma^- & \frac{\Lambda}{\sqrt{6}} - \frac{\Sigma^0}{\sqrt{2}} & n \\ \Xi^- & \Xi^0 & -\frac{2\Lambda}{\sqrt{6}} \end{pmatrix} \quad (8)$$

In order to obtain baryon magnetic moments and the strange magnetic radius one studies vector current matrix elements in SU(3) HBChPT according to

$$J_\mu^{(i)} = \frac{1}{N_1 N_2} \bar{u}(p') P_v^+ \left[ v_\mu G_E^{(i)}(q^2) + [S_\mu, S_\nu] \frac{q^\nu}{m} G_M^{(i)}(q^2) \right] P_v^+ u(p) \quad (9)$$

where  $q^2 = (p' - p)^2$  is the invariant momentum transfer squared and  $m = 1151$  MeV is the average mass of the baryon octet. The quantities  $G_{E,M}^{(i)}(q^2)$  are the electric and magnetic Sachs form factors. Their relation to the Dirac and Pauli form factors  $F_1^{(i)}(q^2)$  and  $F_2^{(i)}(q^2)$  can be found in [15]. The superscript  $i$  denotes the type of current one is interested in:

$$J_\mu^{(\text{em})} := \langle B | \frac{2}{3} \bar{u} \gamma_\mu u - \frac{1}{3} \bar{d} \gamma_\mu d - \frac{1}{3} \bar{s} \gamma_\mu s | B \rangle = \frac{1}{2} J_\mu^{(3)} + \frac{1}{2\sqrt{3}} J_\mu^{(8)}, \quad (10)$$

$$J_\mu^{(s)} := \langle B | \bar{s} \gamma_\mu s | B \rangle = \frac{1}{3} J_\mu^{(0)} - \frac{1}{\sqrt{3}} J_\mu^{(8)}. \quad (11)$$

From an experimental point of view, in addition to the electromagnetic matrix elements one considers the neutral current which couples to the  $Z^0$  and which is of the form

$$J_\mu^{(Z)} := \langle B | \bar{u}_L \gamma_\mu u_L - \bar{d}_L \gamma_\mu d_L - 2 \sin^2 \theta_w \left( \frac{2}{3} \bar{u} \gamma_\mu u - \frac{1}{3} \bar{d} \gamma_\mu d - \frac{1}{3} \bar{s} \gamma_\mu s \right) | B \rangle. \quad (12)$$

Since there are three active degrees of freedom, by combining electromagnetic measurements on the neutron and proton with parity-violating electron-proton scattering results one can isolate the matrix element of the strange quark —  $\langle B | \bar{s} \gamma_\mu s | B \rangle$  — and determine the corresponding strangeness form factors.

The magnetic Sachs form factors have the following Taylor expansion around  $q^2 = 0$  from which one can immediately extract magnetic moments and the strange magnetic radius:

$$G_M^{(\text{em})}(q^2) = \mu^{(\text{em})} + \mathcal{O}(q^2) \quad (13)$$

$$G_M^{(s)}(q^2) = \mu^{(s)} + \frac{1}{6} \langle r_{M,s}^2 \rangle \cdot q^2 + \mathcal{O}(q^4). \quad (14)$$

As an extension of our examination of baryon properties we include intermediate states of the baryon decuplet. The dynamics of the decuplet is contained in the Lagrangian [17, 18]

$$\mathcal{L} = -\bar{T}^\mu i v \cdot D T_\mu + \frac{C}{2} (\bar{T}^\mu u_\mu B + \bar{B} u_\mu T^\mu) + H \bar{T}^\mu S_\nu u^\nu T_\mu + \Delta \bar{T}^\mu T_\mu \quad (15)$$

with

$$D_\nu T_{abc}^\mu = \partial_\nu T_{abc}^\mu + (\Gamma_\nu)_a^d T_{dbc}^\mu + (\Gamma_\nu)_b^d T_{adc}^\mu + (\Gamma_\nu)_c^d T_{abd}^\mu - i T_{abc}^\mu \text{Tr}(v_\nu^{(0)}) \quad (16)$$

$$\bar{T} A B = \bar{T}_{jkl} A^j{}_m B^k{}_n \epsilon^{lmn}, \quad \bar{B} A T = \bar{B}^n{}_k A^m{}_j T^{jkl} \epsilon_{lmn}, \quad (17)$$

$$\bar{T} A T = \bar{T}_{jkl} A^j{}_m T^{mkl}. \quad (18)$$

The fields  $T_{abc}^\mu$  are totally symmetric in the indices  $a$ ,  $b$ , and  $c$ . Their relation to the physical states can be found in ref. [19]. The quantity  $\Delta$  that arises in the last term of eqn. (15) is the difference between the average mass of the decuplet ( $m = 1382$  MeV) and the average mass of the octet ( $m = 1151$  MeV), hence  $\Delta = 231$  MeV. The value for the octet-decuplet coupling is taken to be  $C = -3/2$ , see ref. [14]. Having set our formalism and notation, we now proceed to our calculation.

### 3 Chiral Corrections to $\langle r_{M,s}^2 \rangle$

We have repeated the calculation of the strange magnetic form factor of the proton [1]. In order to address the issue of long vs. short distance contributions we performed the calculations utilizing a momentum space regulator in the loop integral. This technique, often called long distance regularization, has been explored previously in [7]. When the renormalization of the low energy parameters is properly performed, this method reproduces exactly the results of dimensional regularization when the meson masses are small, or equivalently in the limit that the cutoff parameter  $\Lambda$  is taken to infinity. However at finite  $\Lambda$ , the method only admits long distance contributions — *i.e.*, those with  $\delta r > 1/\Lambda$  — since shorter distance contributions are excised by the cutoff. This procedure then provides a diagnostic of how much of the final result comes from long distance physics.

The strange magnetic radius is defined by  $\langle r_{M,s}^2 \rangle = 6 \cdot dG_M^{(s)}(q^2)/dq^2|_{q^2=0}$  and there exists a single diagram with octet baryons and pseudo-Goldstone bosons as intermediate states that contributes to it—*cf.* Figure 1a. When one also includes decuplet baryons as intermediate states there exists an additional diagram as shown in Figure 1b. Throughout, we will work in the Breit frame where  $v \cdot q = 0$ [15].

For both diagrams there is a single generic loop integral which contributes to the strange magnetic form factor at order  $\mathcal{O}(p^3)$ . Before regularization it reads

$$i \int \frac{d^4 k}{(2\pi)^4} \frac{k_\mu k_\nu}{(-v \cdot k - \Delta + i\epsilon)(k^2 - M^2 + i\epsilon)((k+q)^2 - M^2 + i\epsilon)} = I(M, q^2, \Delta) g_{\mu\nu} + \dots \quad (19)$$

and the only term contributing to the strange magnetic form factor is the piece proportional to  $g_{\mu\nu}$ . The parameter  $\Delta = M_\Delta - M_N$  is non-zero only for the diagram with decuplet intermediate states. Since we are primarily discussing the strange magnetic radius we expand  $I(M, q^2, \Delta)$  in powers of

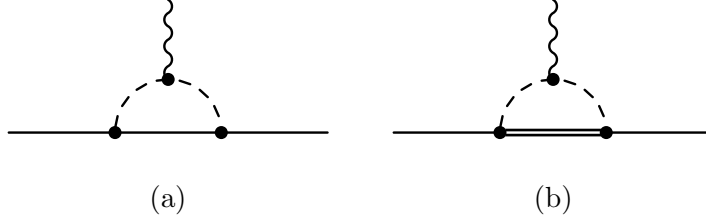


Figure 1: Feynman diagrams contributing to the strange magnetic radius at  $\mathcal{O}(p^3)$ . Solid lines are octet baryons, dashed lines are pseudogoldstone bosons and double lines are decuplet baryons.

$q^2$ —

$$I(M, q^2, \Delta) = I_0(M, \Delta) + I_1(M, \Delta) q^2 + \dots \quad (20)$$

Then  $I_1(M, \Delta)$ , the part proportional to  $q^2$ , is the piece that enters the calculation of  $\langle r_{M,s}^2 \rangle$ .

For simplicity let us first consider only octet baryons as intermediate states so that  $\Delta = 0$ . In dimensional regularization we find

$$I_1^{d.r.}(M, 0) = \frac{1}{16\pi^2} \left( -\frac{\pi}{12M} \right) = -\frac{1}{192\pi M} \quad (21)$$

When applying a dipole regulator for the diagrams in Fig. 1 we associate a monopole form factor with each internal meson line with the respective momenta  $k$  and  $k+q$ —*i.e.*, we regularize the integral of Eq. (19) by multiplying it by a factor

$$\left( \frac{-\Lambda^2}{k^2 - \Lambda^2 + i\epsilon} \right) \left( \frac{-\Lambda^2}{(k+q)^2 - \Lambda^2 + i\epsilon} \right), \quad (22)$$

obtaining

$$I_1^\Lambda(M, 0) = I_1^{d.r.}(M, 0) \cdot X\left(\frac{M}{\Lambda}\right) = -\frac{1}{192\pi M} \cdot X\left(\frac{M}{\Lambda}\right) \quad (23)$$

with

$$X(x) = \frac{1 + \frac{14}{5}x + x^2}{(1+x)^5}. \quad (24)$$

Our result for the strange magnetic radius without decuplet contributions is then

$$\begin{aligned} \langle r_{M,s}^2 \rangle &= -\frac{m(5D^2 - 6DF + 9F^2)}{48\pi M_K F_\phi^2} \cdot X\left(\frac{M_K}{\Lambda}\right) \\ &= \langle r_{M,s,\text{dim.reg.}}^2 \rangle \cdot X\left(\frac{M_K}{\Lambda}\right) = -0.162 \text{ fm}^2 \cdot X\left(\frac{M_K}{\Lambda}\right). \end{aligned} \quad (25)$$

We observe then that integration over the loop in the presence of the cutoff yields the factor  $X(\frac{M}{\Lambda})$ , which has the property  $X(0) = 1$ . This means that as the cutoff goes to infinity, or equivalently as the mass gets small, we recover the dimensional regularization result. Furthermore, the limit  $X(\infty) = 0$  expresses our expectation that for infinitely heavy intermediate masses there is *no* contribution, since such states decouple [8].

This calculation allows us to estimate how much of the result arises from long-distance physics. We do this by comparing the answer for a given cutoff to the answer for infinite cutoff. The ratio of these two numbers yields the fraction of the dimensional regularization result that comes from loop momenta below the cutoff, or equivalently from distance scales larger than  $1/\Lambda$ . We exhibit the cutoff-dependence of the strange magnetic radius in Fig. 2, and quote the ratio to that of dimensional regularization in Table 1. We observe that very little of the dimensional regularization result comes from long distance scales. Indeed, for a reasonable cutoff value of 600 MeV, less than 20% of the dimensional regularization result is obtained. This result suggests that even though the strange magnetic radius is uniquely predicted in  $\mathcal{O}(p^3)$  heavy baryon chiral perturbation theory, using the physical value of the kaon mass, most of the dimensionally regularized result comes from distance scales so small that the effective field theory is not believable.

| $\Lambda/\text{MeV}$  | 300    | 400    | 500    | 600    | 700    | 1000   |
|---|--------|--------|--------|--------|--------|--------|
| $\langle r_{M,s}^2 \rangle_8 / \text{fm}^2$                                 | -0.010 | -0.017 | -0.025 | -0.032 | -0.039 | -0.057 |
| $\frac{\langle r_{M,s}^2 \rangle_8}{\langle r_{M,s,d.r.}^2 \rangle_8}$      | 0.064  | 0.107  | 0.152  | 0.197  | 0.240  | 0.352  |
| $\langle r_{M,s}^2 \rangle_{8+10} / \text{fm}^2$                            | -0.008 | -0.014 | -0.019 | -0.025 | -0.030 | -0.043 |
| $\frac{\langle r_{M,s}^2 \rangle_{8+10}}{\langle r_{M,s,d.r.}^2 \rangle_8}$ | 0.052  | 0.085  | 0.119  | 0.153  | 0.184  | 0.264  |

Table 1:  $\langle r_{M,s}^2 \rangle$  for different values of  $\Lambda$  using octet only and octet plus decuplet intermediate states.



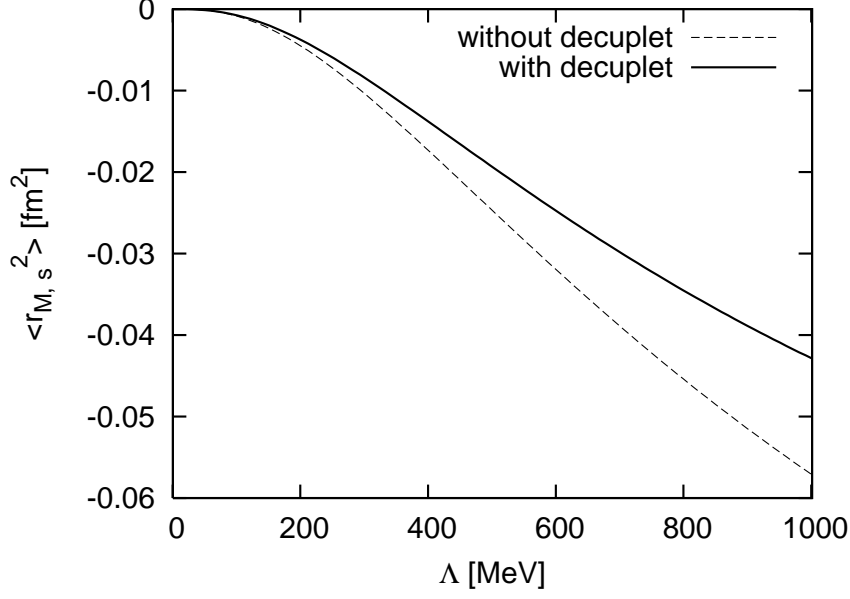


Figure 2: Strange magnetic radius squared with (solid) and without (dashed) inclusion of decuplet loops.

We have also studied the effects of including the decuplet intermediate states and find

$$\langle r_{M,s}^2 \rangle = \langle r_{M,s}^2 \rangle^{octet} + \frac{2mC^2}{(4\pi F_\phi)^2} A^{(1)}(M_K, \Lambda, \Delta) \quad (26)$$

with the octet part  $\langle r_{M,s}^2 \rangle^{octet}$  as given in Eq. (25) and the decuplet loop function

$$\begin{aligned}
A^{(1)}(M, \Lambda, \Delta) = & \\
\Lambda^4 & \left[ \frac{\Delta(-8\Delta^2 + 7M^2 + 7\Lambda^2)}{15(M^2 - \Lambda^2)^4} - \frac{2\Delta(8\Delta^4 + 15M^2\Lambda^2 - 10\Delta^2(M^2 + \Lambda^2))}{15(M^2 - \Lambda^2)^5} \ln \frac{M^2}{\Lambda^2} \right. \\
& + \left( \frac{1}{12(M^2 - \Delta^2)(M^2 - \Lambda^2)^2} - \frac{4(M^2 - \Delta^2)(4\Delta^2 + M^2 - 5\Lambda^2)}{15(M^2 - \Lambda^2)^5} \right) F(M, \Delta) \\
& \left. + \left( \frac{1}{12(\Lambda^2 - \Delta^2)(M^2 - \Lambda^2)^2} + \frac{4(\Lambda^2 - \Delta^2)(4\Delta^2 + \Lambda^2 - 5M^2)}{15(M^2 - \Lambda^2)^5} \right) F(\Lambda, \Delta) \right] \quad (27)
\end{aligned}$$

where

$$F(M, \Delta) = \begin{cases} \sqrt{M^2 - \Delta^2} \left( \pi - 2 \operatorname{Arctan} \frac{\Delta}{\sqrt{M^2 - \Delta^2}} \right) & \text{for } |M| > |\Delta| \\ \sqrt{\Delta^2 - M^2} \ln \frac{\Delta - \sqrt{\Delta^2 - M^2}}{\Delta + \sqrt{\Delta^2 - M^2}} & \text{for } |M| \leq |\Delta| \end{cases} \quad (28)$$

The resulting values for the magnetic strangeness radius are quoted in Table 1.

Let us discuss how our results are connected to other research in this topic. We have highlighted the comparison to the leading model-independent result, which counts as order  $p^3$  in the chiral expansion[1]. The long-distance portion of the one loop integral includes not only the order  $p^3$  result but also higher order pieces, since the cut-off loop function contains terms that are formally of all orders in the chiral expansion. When one works to higher order in the chiral expansion, there will be low-energy constants that enter at the next higher orders. These are regularization scheme dependent, and so these constants will not be the same in dimensional regularization and long-distance regularization. In dimensional regularization, the higher order terms can correct for the misleadingly large leading result. Indeed this seems to happen in a recent calculation performed to order  $p^4$  [9]. Although there is an unknown low-energy constant that enters at the next order, which leads to a large uncertainty in the predicted value, the result that is obtained when this constant is set equal to zero is only a quarter of the order  $p^3$  result. This is qualitatively similar to our result, although our mechanism is not strictly of order  $p^4$ . It would be interesting to carry out a full calculation to order  $p^4$  using long-distance regularization throughout. Our result is even more directly connected to the dispersive treatment of the strange radius[1, 10]. The smallness of the dispersive result is related to the distant  $K\bar{K}$  threshold, which is similar to our suppression by the fact that the kaon mass is so heavy that very little of the kaon loop integral is truly long-distance in character.

## 4 Other aspects of the electromagnetic matrix elements

We have also explored the full treatment of the loop corrections to the electromagnetic currents of the octet of baryons. Details can be found in [21].

Here we report one of the interesting results of this treatment—SU(3) breaking in the magnetic moments of the baryons.

One of the early successes of the quark model was the understanding of the magnetic moments of the baryons. Indeed, it is relatively easy to understand the magnitude of the magnetic moments of the neutron and proton in terms of the magnetic moments of the quarks, as well as naturally predicting the ratio  $\mu_N/\mu_P = -2/3$ . For the other baryons one introduces SU(3) breaking by allowing the strange quark to have a different magnetic moment due to its heavier mass (and hence smaller magnetic moment). The  $\Lambda$  magnetic moment is a particularly nice example of this, since in a valence quark model the moment of the  $\Lambda$  is just the moment of the strange quark. Because the strange quark is more massive than the up and down quarks, the  $\Lambda$  magnetic moment is 30% smaller than its SU(3) prediction.

However, the quark model treatment of SU(3) breaking also has some puzzling failures. This has been highlighted by Lipkin [12] using the magnetic moment of the  $\Sigma^+$ . He considers the ratio

$$R = \frac{\mu_{\Sigma^+} - \mu_P}{\frac{1}{3}(\mu_{\Xi^0} - \mu_{\Xi^-})} \quad (29)$$

for which the experimental value is

$$R_{exp} = 1.68 \pm 0.09 \quad (30)$$

In the quark model this ratio is rather directly related to the quark moments

$$R_{QM} = \frac{\mu_d - \mu_s}{\mu_d} \sim 0.3 \quad (31)$$

and it is difficult to modify this ratio in any significant way. Lipkin explores this problem in detail - it seems to be a firm prediction of the quark model. We will refer to this as the  $\Sigma^+$  puzzle. The resolution must come from physics that is beyond the quark model.

It appears that chiral loops help to resolve the  $\Sigma^+$  puzzle. Chiral loop corrections to the magnetic moments have been studied in the past. In an SU(3) chiral perturbation evaluation using dimensional regularization, these loop effects are so large that they essentially destroy the approximate understanding provided by the quark model [13]. The corrections are so big that the chiral expansion has broken down. Previous studies have shown that the use of long-distance regularization, either without [7] or with [14] decuplet fields, reduces the magnitude of the corrections to a manageable level. However, the effect on phenomenology of the long distance part of the loops

was not studied. Here we note that the SU(3) breaking pattern of chiral loops with long-distance regularization helps improve the phenomenology of either SU(3) fits or quark model fits to the moments.

First let us consider the description of the magnetic moments within the chiral expansion. This is a purely symmetry-based method. At tree level, the magnetic moments are described by two SU(3) parameters, which can be called  $b_D$  and  $b_F$ . As described in [7], the diverging powers of the cutoff  $\Lambda$  are absorbed into the renormalized values of these parameters. The residual effects are contained in the loop integrals. Long distance regularization has been developed for this problem elsewhere [7, 14] and we only present the results. At this level of the chiral expansion, we are including only the lowest order SU(3) parameters and the loop integrals. All of the SU(3) breaking is then contained in the loops. Of course, our fits could be further refined by including higher order parameters in the chiral expansion. Such parameters are surely present and would certainly improve the agreement with experiment — with some loss of predictive power. However, we are interested in demonstrating the basic quality of the fit without invoking these extra parameters.

We consider first the case where only the octet baryons are treated in loop diagrams and then the case where the decuplet is included. For the proton and the neutron, the octet results are

$$\begin{aligned} \mu_p^{\text{ren}} = & \quad 1 + b_F^r + \frac{1}{3} b_D^r + \frac{m}{24 \pi F_\phi^2} \times \\ & \quad \left[ \frac{(F + D)^2 \Lambda^4}{(\Lambda + M_\pi)^3} + \frac{2 (D^2 + 3 F^2) \Lambda^4}{3 (\Lambda + M_K)^3} - \frac{(5 D^2 + 6 DF + 9 F^2) \Lambda}{3} \right], \end{aligned} \quad (32)$$

and

$$\mu_n^{\text{ren}} = -\frac{2}{3} b_D^r + \frac{m}{24 \pi F_\phi^2} \left[ -\frac{(F + D)^2 \Lambda^4}{(\Lambda + M_\pi)^3} + \frac{(D - F)^2 \Lambda^4}{(\Lambda + M_K)^3} + 4 DF \Lambda \right], \quad (33)$$

The limit as  $\Lambda \rightarrow \infty$  corresponds to the result of dimensional regularization [20]. The limit  $\Lambda \rightarrow 0$  is equivalent to not including the chiral loops at all. The coefficients for the other amplitudes are well known and are given in the references [13, 7, 14, 20]. In order to pin down the low-energy constants  $b_D^r$  and  $b_F^r$  we perform a least-squares fit to the experimental data, such that the quantity

$$\chi_\sigma^2 := \frac{1}{N} \sum_i \left[ \frac{\mu_i^{\text{ren}} - \mu_i^{\text{exp}}}{\mu_i^{\text{exp}} \cdot (\sigma/100)} \right]^2 \quad (34)$$

| $\Lambda/\text{MeV}$                 | 300    | 400    | 500    | 600    | 700    | 1000   | 1100   | dim. reg. | exp.     |
|--------------------------------------|--------|--------|--------|--------|--------|--------|--------|-----------|----------|
| $b_D^r$                              | 3.085  | 3.305  | 3.498  | 3.667  | 3.818  | 4.178  | 4.276  | 6.114     |          |
| $b_F^r$                              | 1.187  | 1.349  | 1.492  | 1.617  | 1.728  | 1.994  | 2.065  | 3.416     |          |
| $\mu_p^{\text{ren}}$                 | 2.384  | 2.443  | 2.502  | 2.559  | 2.612  | 2.749  | 2.787  | 3.595     | 2.792847 |
| $\mu_n^{\text{ren}}$                 | -1.616 | -1.696 | -1.777 | -1.854 | -1.927 | -2.113 | -2.165 | -3.263    | -1.91304 |
| $\mu_{\Sigma^+}^{\text{ren}}$        | 2.303  | 2.313  | 2.323  | 2.333  | 2.342  | 2.366  | 2.373  | 2.513     | 2.458    |
| $\mu_{\Sigma^-}^{\text{ren}}$        | -0.871 | -0.912 | -0.953 | -0.992 | -1.029 | -1.124 | -1.150 | -1.710    | -1.16    |
| $\mu_{\Lambda}^{\text{ren}}$         | -0.716 | -0.701 | -0.685 | -0.671 | -0.657 | -0.621 | -0.611 | -0.401    | -0.613   |
| $\mu_{\Lambda\Sigma^0}^{\text{ren}}$ | 1.342  | 1.377  | 1.412  | 1.446  | 1.477  | 1.558  | 1.581  | 2.057     | 1.61     |
| $\mu_{\Xi^0}^{\text{ren}}$           | -1.425 | -1.389 | -1.354 | -1.320 | -1.289 | -1.207 | -1.185 | -0.704    | -1.25    |
| $\mu_{\Xi^-}^{\text{ren}}$           | -0.775 | -0.758 | -0.741 | -0.725 | -0.710 | -0.671 | -0.660 | -0.430    | -0.6507  |
| $\chi_{10}^2$                        | 2.795  | 1.987  | 1.327  | 0.837  | 0.504  | 0.211  | 0.274  | 16.332    |          |
| $\chi_{12}^2$                        | 1.941  | 1.380  | 0.922  | 0.581  | 0.350  | 0.146  | 0.190  | 11.342    |          |
| $\chi_{15}^2$                        | 1.242  | 0.883  | 0.590  | 0.372  | 0.224  | 0.094  | 0.122  | 7.259     |          |
| $R$                                  | 0.374  | 0.617  | 0.875  | 1.138  | 1.398  | 2.142  | 2.373  | 11.85     | 1.676    |

Table 2: Least-squares fit to the octet magnetic moments including octet intermediate states. As described in the text, the factors of  $\chi_\sigma^2$  describe the quality of the fit allowing a fractional uncertainty of  $\sigma\%$ .

gets minimized. The sum over  $i$  covers all baryons in Table 2,  $N$  is the total number of magnetic moments and  $\sigma$  is the allowed percental deviation from the experimental value. The quantity  $\chi_\sigma^2$  then contains information about the quality of the fit. Small values of  $\chi_\sigma^2$  (around unity and below) indicate that theory and experiment agree within the considered percental deviation. In Table 2 we show the result of the fits performed for several values of the separation scale  $\Lambda$ .

We see that the fit is reasonable (better than 10% for many values of  $\Lambda$ ) even without any other sources of SU(3) breaking besides the chiral loops. However, the fit with dimensional regularization is very poor. This quantifies the message of [7], that the dimensional regularization result contains a very large short-distance component (corresponding to energies beyond the scale  $\Lambda$ , which upsets the phenomenology of baryons). This big short distance component requires large coefficients from higher orders in the chiral lagrangian if we are to restore a successful phenomenology. In contrast, when only the long-distance parts of loops are included, there is no need for

any additional significant ingredients. We conclude that the chiral loops aid the phenomenology for moderate values of  $\Lambda$ .

This conclusion is reinforced if we include decuplet baryons in the chiral loops. Here again the dimensionally regularized result leads to corrections that upset the phenomenology. Keeping only the long distance portion of the loops, however, will yield modest corrections that help the phenomenology. If we include the decuplet states we have the additional modification of spin 3/2 loops, which include an additional loop function. This leads to the structure:

$$\begin{aligned}
\mu_{\text{tot}}^{\text{ren}} &= Q \left( 1 + \tilde{b}_F^r \right) + \alpha_D \tilde{b}_D^r \\
&- \frac{m}{24 \pi F_\phi^2} \left[ \beta_\pi \frac{\Lambda^4}{(\Lambda + M_\pi)^3} + \beta_K \frac{\Lambda^4}{(\Lambda + M_K)^3} - (\beta_\pi + \beta_K) \Lambda \right] \\
&+ \frac{m C^2}{(4\pi F_\phi)^2} \left[ \beta_\pi^d \cdot A^{(2)}(\Lambda, M_\pi, \Delta) + \beta_K^d \cdot A^{(2)}(\Lambda, M_K, \Delta) \right. \\
&\left. + (\beta_\pi^d + \beta_K^d) \left[ \frac{\pi}{3} \cdot \Lambda - 2 \Delta \ln\left(\frac{\Lambda}{M_K}\right) \right] \right], \tag{35}
\end{aligned}$$

We have renormalized the SU(3) parameters such that in the limit  $\Lambda \rightarrow \infty$  the results correspond to dimensional regularization at a scale  $\mu = m_K$ . The appropriate coefficients are given below, in Table 3, and in refs. [13, 20]. One finds:

$$\tilde{b}_F^r = b_F^r, \quad \tilde{b}_D^r = b_D^r + \frac{m C^2}{(4\pi F_\phi)^2} \left[ \frac{\pi}{3} \cdot \Lambda - 2 \Delta \ln\left(\frac{\Lambda}{M_K}\right) \right], \tag{36}$$

$$\begin{aligned}
A^{(2)}(\Lambda, M, \Delta) &:= \frac{(4 \Delta^2 - \Lambda^2 - 3 M^2) F(\Lambda, \Delta)}{3 (\Lambda^2 - M^2)^3} \cdot \Lambda^4 \\
&- \frac{(4 \Delta^2 - M^2 - 3 \Lambda^2) F(M, \Delta)}{3 (\Lambda^2 - M^2)^3} \cdot \Lambda^4 \\
&- \frac{2 \Delta \{ \Lambda^2 - M^2 + [4 \Delta^2 - 3 (\Lambda^2 + M^2)] \ln\left(\frac{\Lambda}{M}\right) \}}{3 (\Lambda^2 - M^2)^3} \cdot \Lambda^4. \tag{37}
\end{aligned}$$

Again we attempt a least squares fit to the magnetic moments, including the SU(3) invariant parametrization plus the chiral loops. The results are shown in Table 4. The fits are slightly better than the case above. Again dimensional regularization produces large and unwelcome corrections, which would have to be corrected in higher order. For reasonable values of the

| baryon            | $\beta_\pi^d$    | $\beta_K^d$      |
|-------------------|------------------|------------------|
| $p$               | $-4/9$           | $1/9$            |
| $n$               | $4/9$            | $2/9$            |
| $\Sigma^+$        | $1/9$            | $-4/9$           |
| $\Sigma^0$        | $0$              | $-1/3$           |
| $\Sigma^-$        | $-1/9$           | $-2/9$           |
| $\Lambda$         | $0$              | $1/3$            |
| $\Lambda\Sigma^0$ | $-2/(3\sqrt{3})$ | $-1/(3\sqrt{3})$ |
| $\Xi^0$           | $2/9$            | $4/9$            |
| $\Xi^-$           | $-2/9$           | $-1/9$           |

Table 3: Coefficients  $\beta_\pi^d$  and  $\beta_K^d$ .

cutoff, the chiral loops produce modest and welcome corrections, improving on a pure SU(3) analysis, as shown in Table 4.

Now let us turn to the quark model. In a pure valence quark model, the only ingredients are the quark magnetic moments - the hadron magnetic moments are sums of those of the quarks. The appropriate linear combinations are given in many places, such as Table XII-2 of [11]. When we add chiral loops the issue is less straightforward. Here the idea is that quarks provide a model for the short distance physics, and we supplement the quark moments with the effects of the long distance portions of chiral loops. In doing this, we will keep the entire content of the loops - in particular we will not absorb the terms which are linear in  $\Lambda$  into definitions of renormalized parameters as we did when we were implementing the SU(3) based fits. In practical terms then, the quark moments replace the SU(3) parameters in the expressions given above, and we drop the last terms in the expression of Eq 32,33 and 35 as these were introduced in the renormalization procedure. The important new ingredient is that there is now two sources of SU(3) breaking, that of the chiral loops and the different moments of the quarks.

In this case we explore the phenomenology by fitting the proton, neutron and  $\Lambda$  moments exactly in order to determine the  $u, d, s$  magnetic moments, and then looking at the predictions for the other baryon moments. The results are given in Table 5 and Table 6 for the cases of octet intermediate states only and for octet and decuplet intermediate states.

Again we see that a good phenomenological description is produced, with only these ingredients. The overall results provide a good description

| $\Lambda/\text{MeV}$                 | 300    | 400    | 500    | 600    | 700    | 1000   | 1100   | dim. reg. | exp.     |
|--------------------------------------|--------|--------|--------|--------|--------|--------|--------|-----------|----------|
| $\tilde{b}_D^r$                      | 3.915  | 4.058  | 4.210  | 4.358  | 4.499  | 4.864  | 4.967  | 7.206     |          |
| $\tilde{b}_F^r$                      | 1.190  | 1.356  | 1.501  | 1.629  | 1.743  | 2.017  | 2.091  | 3.506     |          |
| $\mu_p^{\text{ren}}$                 | 2.403  | 2.478  | 2.553  | 2.627  | 2.696  | 2.878  | 2.930  | 4.089     | 2.792847 |
| $\mu_n^{\text{ren}}$                 | -1.627 | -1.715 | -1.805 | -1.891 | -1.972 | -2.183 | -2.242 | -3.530    | -1.91304 |
| $\mu_{\Sigma^+}^{\text{ren}}$        | 2.295  | 2.300  | 2.304  | 2.308  | 2.311  | 2.319  | 2.320  | 2.331     | 2.458    |
| $\mu_{\Sigma^-}^{\text{ren}}$        | -0.874 | -0.918 | -0.962 | -1.005 | -1.044 | -1.148 | -1.177 | -1.802    | -1.16    |
| $\mu_{\Lambda}^{\text{ren}}$         | -0.711 | -0.691 | -0.671 | -0.652 | -0.633 | -0.585 | -0.572 | -0.265    | -0.613   |
| $\mu_{\Lambda\Sigma^0}^{\text{ren}}$ | 1.351  | 1.393  | 1.436  | 1.478  | 1.517  | 1.619  | 1.648  | 2.290     | 1.61     |
| $\mu_{\Xi^0}^{\text{ren}}$           | -1.425 | -1.389 | -1.354 | -1.320 | -1.288 | -1.207 | -1.184 | -0.701    | -1.25    |
| $\mu_{\Xi^-}^{\text{ren}}$           | -0.773 | -0.755 | -0.737 | -0.719 | -0.703 | -0.660 | -0.648 | -0.387    | -0.6507  |
| $\chi_{10}^2$                        | 2.660  | 1.794  | 1.108  | 0.629  | 0.342  | 0.344  | 0.541  | 26.194    |          |
| $\chi_{12}^2$                        | 1.848  | 1.246  | 0.769  | 0.437  | 0.238  | 0.239  | 0.376  | 18.191    |          |
| $\chi_{15}^2$                        | 1.182  | 0.797  | 0.492  | 0.280  | 0.152  | 0.153  | 0.241  | 11.642    |          |
| $R$                                  | 0.498  | 0.839  | 1.209  | 1.590  | 1.971  | 3.069  | 3.413  | 16.785    | 1.676    |

Table 4: Least-square fit to the octet magnetic moments with inclusion of decuplet loops.

of the baryon moments. For many values of  $\Lambda$  the quark moments are of a reasonable size. Note that since there can be chiral renormalizations of the individual quark moments, the quark moments need not satisfy the usual relations such as  $\mu_d/\mu_u = -1/2$ . However, for most values of  $\Lambda$  the modifications appear not to be large. Note, however, that for larger values of  $\Lambda$  including decuplet loops, the modifications of the usual relations are over 100%, casting doubt on the phenomenological utility of these cases.

If we return to the  $\Sigma^+$  puzzle we see that the chiral loops have indeed introduced a new component to the magnetic moments that is effective in changing the ratio. The results are given in the bottom lines of Table 5 and Table 6. For example, from the tables with  $\Lambda = 700$  MeV, we find

$$\begin{aligned}
R &= 1.345 && \text{octet only} \\
&= 1.383 && \text{with decuplet}
\end{aligned} \tag{38}$$

The agreement with experiment is acceptable given that we are not including any further sources of SU(3) breaking. The basic message is clear. For reasonable values of the cutoff, the chiral loops readily address some of the puzzles of the quark model. The loops give a mechanism that shifts



| $\Lambda$ [MeV]         | tree   | 300    | 400    | 500    | 600    |
|-------------------------|--------|--------|--------|--------|--------|
| $\mu_u$                 | 1.852  | 1.702  | 1.588  | 1.454  | 1.305  |
| $\mu_d$                 | -0.972 | -0.845 | -0.758 | -0.662 | -0.561 |
| $\mu_s$                 | -0.613 | -0.595 | -0.574 | -0.543 | -0.504 |
| $\mu_p$                 | 2.793  | 2.793  | 2.793  | 2.793  | 2.793  |
| $\mu_n$                 | -1.913 | -1.913 | -1.913 | -1.913 | -1.913 |
| $\mu_\Lambda$           | -0.613 | -0.613 | -0.613 | -0.613 | -0.613 |
| $\mu_{\Sigma^+}$        | 2.673  | 2.629  | 2.602  | 2.575  | 2.548  |
| $\mu_{\Lambda\Sigma^0}$ | 1.630  | 1.603  | 1.586  | 1.568  | 1.550  |
| $\mu_{\Sigma^-}$        | -1.091 | -1.053 | -1.033 | -1.016 | -1.003 |
| $\mu_{\Xi^0}$           | -1.435 | -1.389 | -1.361 | -1.332 | -1.304 |
| $\mu_{\Xi^-}$           | -0.493 | -0.542 | -0.573 | -0.607 | -0.642 |
| $R$                     | 0.381  | 0.581  | 0.728  | 0.903  | 1.107  |

| $\Lambda$ [MeV]         | 700    | 800    | 900    | 1000   | exp.    |
|-------------------------|--------|--------|--------|--------|---------|
| $\mu_u$                 | 1.143  | 0.972  | 0.792  | 0.605  |         |
| $\mu_d$                 | -0.457 | -0.351 | -0.245 | -0.137 |         |
| $\mu_s$                 | -0.458 | -0.405 | -0.347 | -0.284 |         |
| $\mu_p$                 | 2.793  | 2.793  | 2.793  | 2.793  | 2.793   |
| $\mu_n$                 | -1.913 | -1.913 | -1.913 | -1.913 | -1.913  |
| $\mu_\Lambda$           | -0.613 | -0.613 | -0.613 | -0.613 | -0.613  |
| $\mu_{\Sigma^+}$        | 2.524  | 2.500  | 2.479  | 2.459  | 2.458   |
| $\mu_{\Lambda\Sigma^0}$ | 1.532  | 1.514  | 1.498  | 1.481  | 1.61    |
| $\mu_{\Sigma^-}$        | -0.993 | -0.988 | -0.986 | -0.987 | -1.16   |
| $\mu_{\Xi^0}$           | -1.277 | -1.251 | -1.227 | -1.204 | -1.25   |
| $\mu_{\Xi^-}$           | -0.677 | -0.711 | -0.745 | -0.779 | -0.6507 |
| $R$                     | 1.345  | 1.623  | 1.954  | 2.356  | 1.676   |

Table 5: Quark model results for the magnetic moments, including only octet loops.

| $\Lambda$ [MeV]         | 300    | 400    | 500    | 600    | 700    |
|-------------------------|--------|--------|--------|--------|--------|
| $\mu_u$                 | 1.687  | 1.561  | 1.412  | 1.247  | 1.068  |
| $\mu_d$                 | -0.825 | -0.718 | -0.598 | -0.468 | -0.330 |
| $\mu_s$                 | -0.590 | -0.562 | -0.522 | -0.469 | -0.407 |
| $\mu_p$                 | 2.793  | 2.793  | 2.793  | 2.793  | 2.793  |
| $\mu_n$                 | -1.913 | -1.913 | -1.913 | -1.913 | -1.913 |
| $\mu_\Lambda$           | -0.613 | -0.613 | -0.613 | -0.613 | -0.613 |
| $\mu_{\Sigma^+}$        | 2.607  | 2.563  | 2.519  | 2.475  | 2.434  |
| $\mu_{\Lambda\Sigma^0}$ | 1.610  | 1.601  | 1.592  | 1.587  | 1.583  |
| $\mu_{\Sigma^-}$        | -1.018 | -0.964 | -0.903 | -0.837 | -0.767 |
| $\mu_{\Xi^0}$           | -1.398 | -1.379 | -1.361 | -1.345 | -1.332 |
| $\mu_{\Xi^-}$           | -0.526 | -0.540 | -0.550 | -0.555 | -0.554 |
| $R$                     | 0.640  | 0.821  | 1.014  | 1.205  | 1.383  |

| $\Lambda$ [MeV]         | 800    | 900    | 1000   | 1100   | exp.    |
|-------------------------|--------|--------|--------|--------|---------|
| $\mu_u$                 | 0.878  | 0.680  | 0.474  | 0.263  |         |
| $\mu_d$                 | -0.188 | -0.041 | 0.110  | 0.263  |         |
| $\mu_s$                 | -0.335 | -0.255 | -0.168 | -0.074 |         |
| $\mu_p$                 | 2.793  | 2.793  | 2.793  | 2.793  | 2.793   |
| $\mu_n$                 | -1.913 | -1.913 | -1.913 | -1.913 | -1.913  |
| $\mu_\Lambda$           | -0.613 | -0.613 | -0.613 | -0.613 | -0.613  |
| $\mu_{\Sigma^+}$        | 2.395  | 2.359  | 2.326  | 2.296  | 2.458   |
| $\mu_{\Lambda\Sigma^0}$ | 1.582  | 1.583  | 1.586  | 1.591  | 1.61    |
| $\mu_{\Sigma^-}$        | -0.695 | -0.621 | -0.545 | -0.468 | -1.16   |
| $\mu_{\Xi^0}$           | -1.322 | -1.314 | -1.308 | -1.304 | -1.25   |
| $\mu_{\Xi^-}$           | -0.547 | -0.536 | -0.520 | -0.500 | -0.6507 |
| $R$                     | 1.540  | 1.672  | 1.776  | 1.854  | 1.676   |

Table 6: Quark model results for the magnetic moments including octet and decuplet loops.

the  $\Sigma^+$  ratio in the right direction without destroying the general level of agreement between theory and experiment. A conceptually simple way to understand the baryon magnetic moments then starts with quark moments and augments these with modest corrections from the chiral loops. The  $\Sigma^+$  puzzle is likely an indicator of the presence of the chiral loops.

## 5 Conclusions

We have found that the long distance part of the kaon loop calculation is a relatively small fraction of the result that has been reported as the consequence of chiral perturbation theory [1]. Because the chiral theory is meant to be an effective field theory valid only in the long distance regime, the short distance parts of the calculation are spurious and are not true consequences of QCD. Chiral loops, when treated including all scales, produce corrections that are so large that they disrupt standard phenomenology. However, the need for such loops is clear and they should not be totally discarded. We therefore propose to keep only the long distance contributions as model-independent the consequences of the kaon loop.

This work resolves the discrepancy between the chiral studies and dispersive calculations of the same quantity, which also suggest a considerably smaller strange radius. If we look carefully at the dispersive calculation, we conclude that the reason is the same as found above—the kaon mass is large and does not contribute to the low energy (and therefore trustworthy) component of the dispersive integral.

## Acknowledgements

This manuscript has been produced for a memorial volume for Dubravko Tadić. During his career Dubravko worked on various aspects of the chiral quark model, and had a deep interest in quarks and chiral physics. We would like to thank Bastian Kubis, Martin Mojžiš and Thomas Mannel for many useful discussions. This work was supported in part by the National Science Foundation under award PHY02-44801 and by ERDF funds from the European Commission. This work was also supported by the “Studienstiftung des deutschen Volkes” (Germany) and the “Schweizerischer Nationalfond” (Switzerland).

## References

- [1] T. R. Hemmert, U. G. Meissner and S. Steininger, “Strange magnetism in the nucleon,” *Phys. Lett. B* **437**, 184 (1998) [arXiv:hep-ph/9806226]; T. R. Hemmert, B. Kubis and U. G. Meissner, “Strange chiral nucleon form factors,” *Phys. Rev. C* **60**, 045501 (1999) [arXiv:nucl-th/9904076].
- [2] M.J. Ramsey-Musolf and H.-W. Hammer, and D. Drechsel, “Nucleon strangeness and unitarity,” *Phys. Rev.* **D55**, 2741 (1997); M.J. Ramsey-Musolf and H.-W. Hammer, “K N scattering and the nucleon strangeness radius,” *Phys. Rev. Lett.* **80**, 2539 (1998); “Spectral content of isoscalar nucleon form factors,” *Phys. Rev.* **C60**, 045205 and 024205 (1999).
- [3] D. Spayde et al., “The strange quark contribution to the proton’s magnetic moment,” *Phys. Lett.* **B583**, 79 (2004); T.M. Ito et al., “Parity-violating electron deuteron scattering and the proton’s neutral weak axial vector form factor,” *Phys. Rev. Lett.* **92**, 102003 (2004).
- [4] K.A. Aniol et al., “Parity-violating electroweak asymmetry in e(pol.) p scattering,” *Phys. Rev.* **C69**, 065501 (2004).
- [5] D.H. Beck and R.D. McKeown, ‘Parity-violating electron scattering and nucleon structure,’ *Ann. Rev. Nucl. Part. Sci.* **51**, 189 (2001); D.H. Beck and B.R. Holstein, ‘Nucleon structure and parity-violating electron scattering,’ *Int. J. Mod. Phys.* **E10**, 1 (2001).
- [6] F.E. Maas et al., “Measurement of strange quark contributions to the nucleon’s form factors at  $Q^{*2} = 0.230\text{-(GeV/c)}^{*2}$ ,” *Phys. Rev. Lett.* **93**, 022002 (2004).
- [7] J. F. Donoghue and B. R. Holstein, “Improving the convergence of SU(3) baryon chiral perturbation theory,” arXiv:hep-ph/9803312; J. F. Donoghue, B. R. Holstein and B. Borasoy, “SU(3) baryon chiral perturbation theory and long distance regularization,” *Phys. Rev. D* **59**, 036002 (1999) [arXiv:hep-ph/9804281].
- [8] T. Appelquist and J. Carazzone, “Infrared Singularities And Massive Fields,” *Phys. Rev.* **D11**, 2856 (1975).
- [9] H. W. Hammer, S. J. Puglia, M. J. Ramsey-Musolf and S. L. Zhu, “What do we know about the strange magnetic radius?,” *Phys. Lett. B* **562**, 208 (2003) [arXiv:hep-ph/0206301].

- [10] H. W. Hammer, “Nucleon strangeness in dispersion theory,” arXiv:hep-ph/0301129.
- [11] J. F. Donoghue, E. Golowich and B. R. Holstein, “Dynamics of the standard model,” Cambridge Monogr. Part. Phys. Nucl. Phys. Cosmol. **2**, 1 (1992).
- [12] H. J. Lipkin, “A Model Independent Analysis Of Experimental Baryon Magnetic Moments,” Phys. Rev. D **24**, 1437 (1981).
- [13] E. Jenkins, M. E. Luke, A. V. Manohar and M. J. Savage, “Chiral perturbation theory analysis of the baryon magnetic moments,” Phys. Lett. B **302**, 482 (1993) [Erratum-ibid. B **388**, 866 (1996)] [arXiv:hep-ph/9212226].
- [14] B. Borasoy, B. R. Holstein, R. Lewis and P. P. A. Ouimet, “Long distance regularization in chiral perturbation theory with decuplet fields. ((U)),” Phys. Rev. D **66**, 094020 (2002) [arXiv:hep-ph/0210092].
- [15] V. Bernard, H. Fearing, T. R. Hemmert and Ulf-G. Meißner, “The form factors of the nucleon at small momentum transfer,” Nucl. Phys. A **635**, 121, (1998) [arXiv:hep-ph/9801297].
- [16] N. Fettes, Ulf-G. Meißner, M. Mojžiš and S. Steininger, “The chiral effective pion nucleon Lagrangian of order  $p^{*4}$ ,” Annals Phys. **283**, 273, (2000), (E) **288**, 249 (2001) [arXiv:hep-ph/0001308].
- [17] E. Jenkins, A. V. Manohar, M. Luke and M. Savage, “Chiral perturbation theory analysis of the baryon magnetic moments,” Phys. Lett. B **302**, 482, (1993) [arXiv:hep-ph/9212226].
- [18] M. A. Luty and M. White “The Role of decuplet states in baryon chiral perturbation theory,” [arXiv:hep-ph/9305203].
- [19] M. N. Butler, M. J. Savage and R. P. Springer, “Strong and electromagnetic decays of the baryon decuplet,” Nucl. Phys. B **399**, 69, (1993) [arXiv:hep-ph/9211247].
- [20] B. Kubis, T. R. Hemmert and Ulf-G. Meißner, “Baryon form factors,” Phys. Lett. B **456**, 240, (1999) [arXiv:hep-ph/9903285].
- [21] T. Huber, “Chiral nucleon form factors and long distance regularization,” Master Thesis, University of Massachusetts, Amherst, (2002);

T. Huber, “Baryon form factors and baryon decays in Chiral Perturbation Theory,” Diploma Thesis, Universität Karlsruhe, (2003) A. Ross “Applications and Techniques of Long Distance Regularization in Chiral Perturbation Theory” Master’s thesis University of Massachusetts (2003).